Effective Surface Area of Hardened Cement Pastes

S. Tada[1], H. Utsumi[2]

[1]*Texte, Inc. Tokyo, Japan*; [2]*Chiba Institute of Technology, Narashino, Japan*

1. Introduction

Specific surface area of hardened cement paste changes with hydration and subsequent carbonation, reflecting the change in microstructure of hardened body. Determination of specific surface area is thus essential in studying the degree of hydration, quality evaluation and durability of concrete. Determination of the specific surface area has been performed mainly with BET gas adsorption, small angel X-ray scattering SAXS, small angle neutron scattering SANS, helium pycnometry and mercury porosimetry. The BET gas adsorption model [1] assumes multilayer adsorption of gas molecule on a molecularly smooth surface. Effects of the opposite surface are not taken into account allowing unlimited number of adsorbed molecular layer and hence the capillary condensation cannot be described. The assumption of the molecularly smooth surface may not work out when the same molecule as being adsorbed comprises the near-surface region of the solid. The small angel X-ray scattering [2] and the small angle neutron scattering [3] do not require drying of the specimen whereas they are not easily available. The helium pycnometry [4] is a simple method to determine a specific surface area by extracting the specimen volume at the monolayer adsorption of water from that at the standard drying, while the relative humidity that gives the monolayer adsorption state is questionable. The mercury porosimetery can wet the entire capillary space with mercury under the maximum pressures of the currently available equipment, but excludes very fine pores accessible only by water molecule. Thus it is noted that very few methods that are currently available can determine the specific surface area with ease of execution, broad applicable range and rigor of underlying principle.

In this study, we derived the general from of Kiselev-Brunauer equation on the basis of rigorous thermodynamics and proposed the effective surface area, a general concept of specific surface area applicable from monomolecular, monolayer to capillary condensation. The effective surface area was determined in experiments of water vapor adsorption. Fractal dimension of the effective surface area was also obtained from the water vapor adsorption and compared with those obtained by other methods to verify the universal applicability of the effective surface area.

2. Thermodynamics of water vapor adsorption

A system of water vapor adsorption is shown in Fig. 1 where an amount of water adsorbed isothermally on a specimen with a change in relative

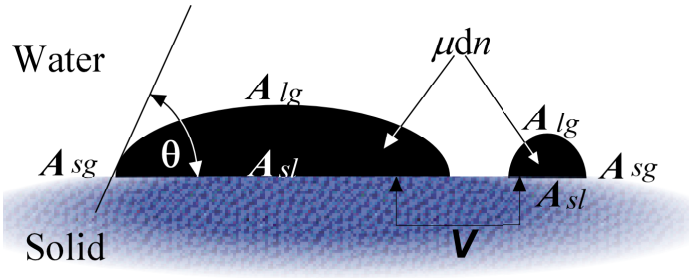

Fig. 1 Definition of the thermodynamic system

pressure *h* is determined. The thermodynamic system, composed only of water (liquid phase l and gas phase g) in a porous solid, is an open system allowing incoming water molecules associated with a change in relative pressure. The volume of the system *V* increases associated with changes in interfacial free energies between adsorbed water and solid (sl), water vapor and solid (sg) and adsorbed water and water vapor (lg). The total differential of the Gibbs free energy *G* (=*F*+*PV*) [5] of the system is given by

$$dG = -SdT + VdP + \mathrm{f}_{sg}dA_{sg} + \mathrm{f}_{sl}dA_{sl} + \mathrm{f}_{\mathrm{lg}}dA_{\mathrm{lg}} + \mathrm{m}_{w}dn\,, \tag{1}$$

where *S* is entropy of the system, *P* is pressure of the system, A_{ij} is interfacial area and f_{ij} is interfacial free energy. The chemical potential of water in the gas phase m_{w} with respect to the isothermal free bulk water is given by *RT*ln(*h*) where *R* is the gas constant of water vapor. Change in the amount of water d*n* entering the system is given by d*n*=d*V*/*v* where *v* is specific volume of water.
When the system becomes an adsorption equilibrium (d*G*=0) isothermally (d*T*=0) under normal pressure (d*P*=0), only reversible work terms remain in the Eq. 1,

$$\mathrm{f}_{sg}\mathrm{d}A_{sg} + \mathrm{f}_{sl}\mathrm{d}A_{sl} + \mathrm{f}_{\mathrm{lg}}\mathrm{d}A_{\mathrm{lg}} + RT\ln(h)\cdot\frac{\mathrm{d}V}{v} = 0\,. \tag{2}$$

Young's equation gives

$$\mathrm{f}_{sg} = \mathrm{f}_{sl} + \mathrm{f}_{\mathrm{lg}}\cos\mathrm{q}_{w}\,, \tag{3}$$

where q_{w} is contact angle between water and solid.
Substitution of Eq. 3 to Eq. 2 and some rearrangements result in

$$\mathrm{f}_{\mathrm{lg}}\mathrm{d}\left(A_{\mathrm{lg}} - A_{sl}\cos\mathrm{q}_{w}\right) + RT\ln(h)\cdot\frac{\mathrm{d}V}{v} = 0\,. \tag{4}$$

At the initial stage of the adsorption, *V*=0, A_{lg}=0 and A_{sl}=0 are supposed and

definite integration of Eq. 4 over the interval gives

$$\mathsf{f}_{\mathrm{lg}} \int_0^{A_{ig}} dA_{\mathrm{lg}} - \mathsf{f}_{\mathrm{lg}} \cos\mathsf{q}_w \int_0^{A_{sl}} dA_{sl} + \frac{RT\ln(h)}{v} \int_0^{V} \mathrm{d}V = 0\,, \tag{5}$$

and a rearrangement leads to the equation of state of water including the adsorption stage lower than monomolecular adsorption,

$$\mathsf{f}_{\mathrm{lg}} \left[A_{\mathrm{lg}} - A_{sl} \cos\mathsf{q}_w \right] = -\frac{RT\ln(h)}{v} \cdot V\,. \tag{6}$$

At the beginning of the water vapor adsorption, V=0 corresponds to a zero left hand side (A_{lg}=0 and A_{sl} =0), while at the end of adsorption when h approaches to 1, the left hand side of Eq. 6 may converge to a finite value of A_{lg} that may corresponds to the liquid-gas interface of the specimen.
The relationship between effective surface area A=A_{lg}-A_{sl}cosq$_w$ (m^2/g) and moisture content (m^3/g) can be obtained by dividing the both sides of Eq. 6 with unit mass. The meaning of A is the net surface area that varies with the progress of adsorption and capillary condensation, and the Eq. 6 is the generalized Kiselev-Brunauer equation [6].
During the derivation of Eq. 6, no particular geometry and relative configuration between adsorbed water film and capillary condensate were assumed. At the early stage of adsorption, adsorbed water molecules may form a cluster configuration prior to the transition to a liquid film. In the later stages of adsorption where the water extends over the capillary condensation region, A_{sg}=0 and dA_{lg}<0 work out and A_{lg} finally approaches to the superficial surface area of a specimen. This surface area is negligibly small compared to the specific surface are of the specimen but a finite value so that A (=A_{lg}-A_{sl}cosq$_w$) will not reach zero at the full saturation.
The effective surface area was originally presented by Everett and Haynes [7] with a different approach, but its applicable ranges and experimental verification were not presented and, as a method of determining specific surface area, comparison with other methods was not shown. One of us showed the effective surface area of autoclaved aerated concrete as a function of relative humidity and that it has a maximum at a lower relative humidity range [8]. In this study, characteristics of the effective surface area are much widely discussed using water vapor adsorption data obtained in our previous study [9].

3. Effective surface area

3.1 Experimental determination of effective surface area

Effective surface area is a net surface area that varies during adsorption and a pore structure parameter obtainable from gas adsorption data without any presupposition for pore geometry.

With surface tension of water f and hydraulic radius *Rh* (= *V*/*A*), the Eq. 6 gives,

$$\frac{RT\ln(h)}{v} = -\frac{\mathrm{f}}{Rh}, \tag{7}$$

where water specific gas constant *R* of 491.5 (J/kgK), absolute temperature *T* of 293.15 (K), specific volume of water of 10^{-3} (m^3/kg) and surface tension of water of 72.75 x 10^{-3} (J/m^2) are adopted.
When a relative pressure *h* and adsorbed volume *V* (m^3) relation is given by a measurement of water vapor sorption isotherm, determination of effective surface area can be approached first by calculating the chemical potential of water as follows,

$$RT\ln(h) = 461.5 \text{ x } 293.15 \text{ x } \ln(h). \tag{8}$$

The hydraulic radius *Rh* is a function of relative pressure *h* and given by

$$Rh = \left(-72.75 \text{ x } 10^{-3} \text{ x } 10^{-3}\right) / RT\ln(h), \tag{9}$$

and the effective surface area *A* (m^2/g) is obtained as *A*=*V*/*Rh* using adsorbed amount *V* (m^3/g) and *Rh* (m).
Relationship between effective surface area of hardened cement pastes and relative humidity (*h* x 100) is shown in Fig. 2. The data of the water vapor sorption isotherm is given in the previous paper [9]. Prior to the first adsorption, specimens were equilibrated in a chamber where a dry air with a dew point temperature of -42°C was flowing 20 liters per minute, and this equilibrium moisture content was defined as the zero moisture content, which approximately corresponds to an oven-dry condition at 90°C.
The dry air with a dew point temperature of -42°C was created with a molecular sieve dryer in which two groups of zeolite 5A adsorb both moisture and atmospheric carbon dioxide and are revived at a temperature of 200°C by turns. We call the drying method hereafter the molecular sieve drying. Relative humidity was generated by mixing the dry air and a saturated air at desired mix proportions. This equipment was calibrated with a chilled-mirror type dew point hygrometer traceable to US standard and the resulting precision was better than plus or minus 1 percent of relative humidity.
With an increase in relative humidity, the effective surface area that is the sum of solid-liquid and liquid-gas interfacial areas increased first and then showed a maximum at a relative humidity of approximately 30 % and decreased subsequently. This tendency was common to all the specimens of different water-cement ratios, while the maximum values became larger with an increase in water-cement ratio.

3.2 Applicable range of effective surface area

In an energetic aspect, the relationship between effective surface area and relative humidity represents a possible area work done by water and the respective pore regions. The changes in interfacial areas corresponding to the change in effective surface area and in relative humidity are illustrated at the side of Fig. 2. Changes in solid-liquid and liquid-gas interfacial areas with the development of adsorption are intuitively shown. A water adsorption process from a very dry condition with almost no water molecules on the solid surface to a slightly adsorbed state is shown in Fig. 2 A. However, depending on the method of drying, very narrow pores accessible only by water molecules may be filled with gel water. In this adsorption stage, the amount of water is not large enough to form a liquid film and the water molecules that selectively adsorbed on an adsorption site may form a hydrogen-bonded cluster configuration, where A_{lg} and A_{sl} are nearly zero and A is almost zero. With a progress of adsorption, A_{lg} increases as shown in Fig. 2 B. When relative humidity approaches to 30 %, the clustered water molecules may form a monolayer by phase transition, where contribution of $A_{sl}\cos\theta_w$ becomes negligible because A_{sl} is 0 though $\cos\theta_w$ becomes 1. This leads to the maximum of A_{lg} and hence the maximum of A. Further progress of adsorption results in the emergence of a capillary-condensed phase as shown in Fig. 2 D, where A_{lg} obviously decreases due to the capillary condensation. Subsequent progress may lead to a very small, infinite but not zero value of A_{lg}, which will probably converge with the apparent surface area of a specimen as remarked above. On the other hand, extrapolation of the curve A into the relative humidity of 0% implies that the effective surface area may vanish. Decrease in

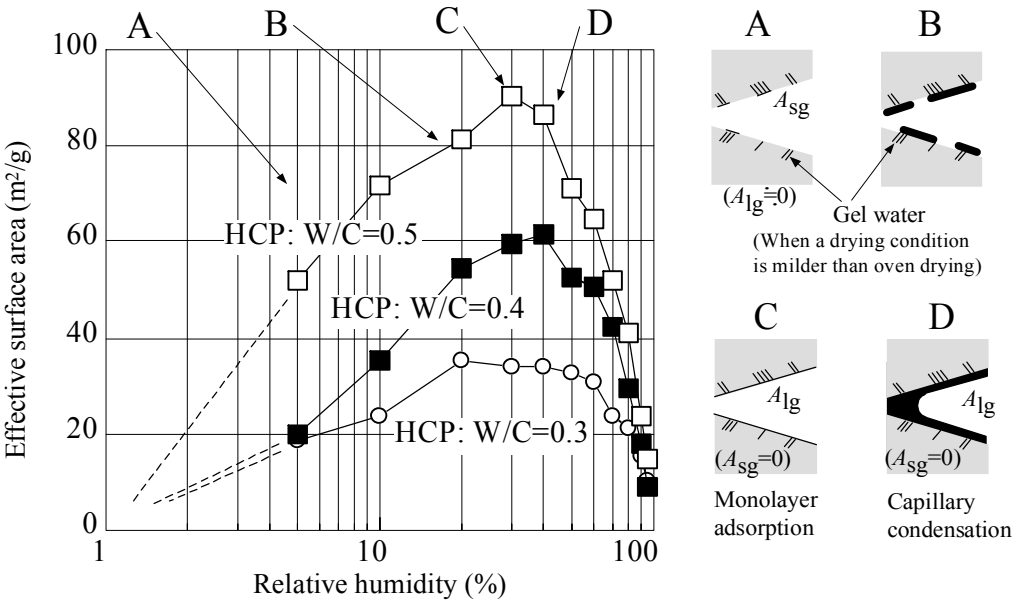

Fig. 2 Effective surface area of hardened cement pastes and its physical meaning

adsorbed water obviously results that A_{lg} and A_{sl} converges with zero and hence A will converge with zero.
As remarked above, one of the important characteristics of the effective surface area is the applicability over the entire adsorption range, from monomolecular adsorption at early stage, monolayer adsorption to the full saturation of pore space.

3.3 Effective surface area and BET specific surface area
Taking the maximum of the effective surface area, the peaks in Fig. 2, as specific surface area of hardened cement paste, these values are plotted against water-cement ratio with other data [4, 10, 11, 12] which used various types of gas and drying conditions in Fig. 3. When water was used as an adsorbate and specimens were subjected to D-drying, the specific surface areas were approximately 200 (m^2/g) regardless of their water-cement ratio. The D-drying partially ejects water molecules that reside in the nano space exclusively available to water, i.e. gel pores, and this results in a violation of BET assumption that the adsorbent surface should be molecularly smooth. Specific surface areas measured by helium pycnometry were approximately 50 (m^2/g) regardless of their water-cement ratio. This may be attributed to the assumption that the water monolayer forms at a relative humidity of 11 percent; the question lies in drying condition and not in molecular size of adsorbing gas. Chemical potentials of water, with respect to the free bulk water, at the nominal zero moisture content employed in each drying method are shown at the right hand side of Fig. 3 to compare their drying conditions.
SAXS, SANS and NMR methods which require no prerequisite drying may be more appropriate for specific surface area determination [2], but its significance is limited because a region that may not be a liquid-solid “interface” is measured.

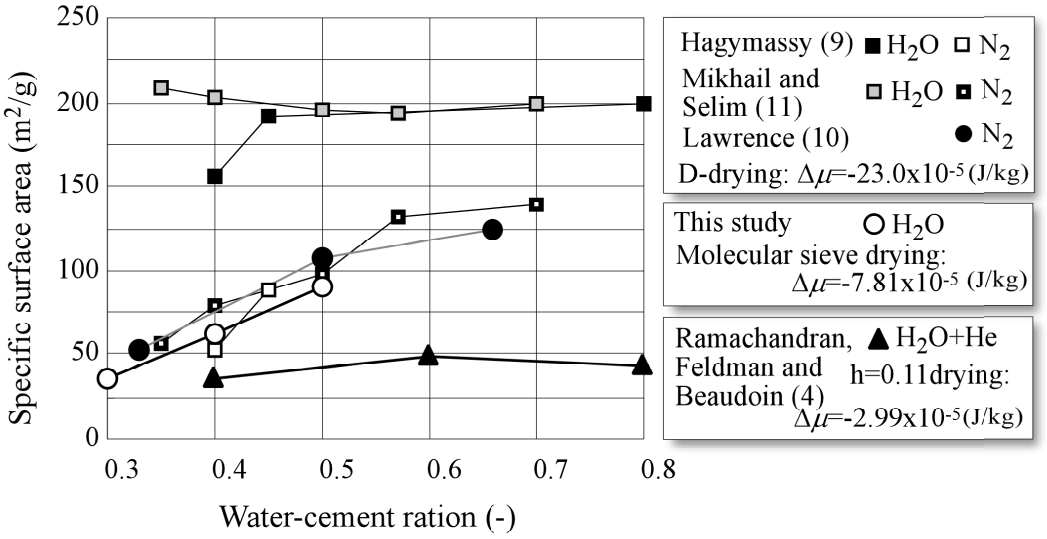

Fig. 3 Specific surface area of hardened cement paste determined with various methods

Depending on the objective of study, a method capable of distinguishing the characteristics of specimen such as water-cement ratio and changes in properties over time can be of significance. The specific surface area measured with water adsorption showed good agreement with that with BET nitrogen adsorption and was able to describe the dependency of specific surface area on water-cement ratio, and hence an appropriate method in this sense. However the conditions of the agreement are limited and depend on the drying condition or nominal zero moisture content of the specimen. Using molecular sieve dryer, this experiment applied dry air of a dew point temperature of -42 °C in a thermostatic chamber at a room temperature, which was nearly equal to an oven-dry at 90 °C. This resulted in the launch of adsorption leaving sufficient amount of gel water in the fine pores and is a similar situation when nitrogen adsorbs on a D-dried surface of hardened cement pastes.
The discrepancy in the measurement of specific surface area is a manifestation of a fractal character of the surface of hardened cement paste rather than the appropriateness in the selection of gas species.

3.4 Effective surface area and surface fractal dimension
Pfiefer and Avnir [13] have presented a unified view on the relationship between specific surface area in materials science and its measurement method by introducing a concept of fractal dimension. Using SAXS, Winslow [14] measured a surface fractal dimension (a noninteger between 2 and 3) of hardened cement paste for the first time. Because it was almost 3.0 regardless of the water-cement ratio, he concluded that the surface of hardened cement paste was highly complex.
Subsequently, the surface fractal dimension has been determined by many authors with a variety of methods. In this study, we determined a surface fractal dimension using the effective surface area and compared those with other methods to verify the universal applicability of the concept of the effective surface area.
Niklasson [15] derived a fractal dimension D of hardened cement paste based on adsorbed volume V (m^3/g) and relative pressure h to a relative humidity range greater than 35 percent.

$$V \propto \left[\ln(1/h)\right]^{(D-3)}. \tag{10}$$

where the yardstick ln(1/h) can be related to Kelvin radius r by ln(h)=-2vf cosq/RTr=-k/r . On the other hand, surface fractal dimension based on specific surface area and pore radius was given by Pfeifer and Avnir [12]. In this study, we interpreted the relation as that between effective surface area A and hydraulic radius Rh.

$$A \propto Rh^{(2-D)}. \tag{11}$$

A least square fit of log(A)=log(k)+(2-D)log(Rh) for the amount of adsorption

Table 1 Fractal dimension of hardened cement pastes (W/C=0.4) determined with various techniques

Author	Method	Fractal dim. D	Note
Häußler *et. al*. [3]	SANS	2.59	
Niklasson [15]	Water vapor adsorption	2.50	W/C=0.465
Beddoe and Lang [16]	SAXS	2.52-2.62	Different types of cement
This study	Water vapor adsorption	2.59	

at relative humidity greater than 35 percent was performed and is shown in Fig. 4. Because the gradient of the lines give (2-D), the surface fractal dimensions of hardened cement pastes with water-cement ratios of 0.3, 0.4 and 0.5 worked out to be 2.44, 2.59 and 2.62 respectively. The fractal dimension determined here is a characteristic of the liquid-gas interfacial area at capillary condensation regions

The measured fractal dimensions of hardened cement paste and those found in literatures are compiled in Table 1. Water-cement ratio of 0.4 was common to all the specimens extracted form the literatures, while the basic formulas for the calculation of fractal dimension were different. No formula was presented in Beddoe and Lang [16] with SAXS. In any event, surface fractal dimensions of hardened cement paste with a water cement ratio of 0.4 ranges from 2.5 to 2.6. The surface fractal dimension based on the effective surface showed no contradiction with those measured with other method for specific surface area.

4. Conclusions

An equation of state of adsorbed water was derived on the basis of rigorous thermodynamics and the effective surface area, a general form of specific

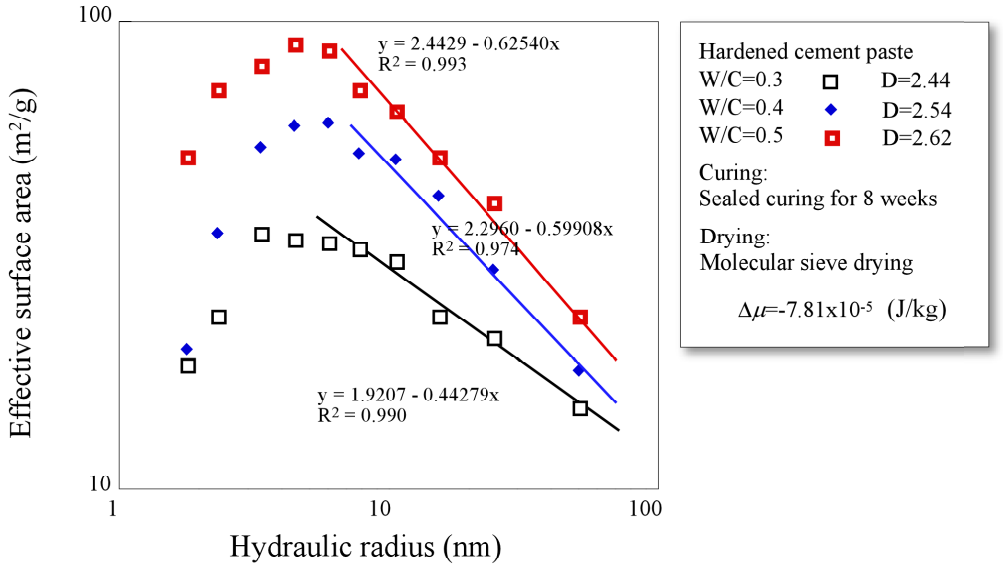

Fig. 4 Fractal dimension of hardened cement pastes by water vapor adsorption

surface area was proposed. The effective surface area can describe a broad range of water biding processes from very early stage of adsorption, monolayer to fully saturated state. The effective surface areas obtained for hardened cement pastes exhibited a good agreement with BET surface area obtained with N_2 adsorption and clear distinction according to the difference in water-cement ratio. It should be noted that the agreement is restricted to the drying condition prior to the water vapor adsorption, i.e. definition of zero moisture content. The dependency of the effective surface area on drying condition is originated probably from nano-micro pore structure of hardened cement paste and requires a further investigation.

References

[1] D. L. Kantro, S. Brunauer, L. E. Copeland, BET surface area - Methods and interpretations, in The Solid-Gas Interface, Ed. by Flood, E. A., Marcel Dekker, Inc. N.Y., 1967, 413-429

[2] J. J. Thomas, H. M. Jennings A. J. Allen, The surface area of hardened cement paste as measured by various techniques, Concrete Science and Engineering, 1 (1999) 45-64

[3] F. Häußler, S. Palzer, A. Eckart, Nanostructural investigations on carbonation of hydrating tricalcium silicate by small angle neutron scattering, LACER (5) (2000) Universität Leipzig

[4] V. S. Ramachandran, R.F. Feldman, J. J. Beaudoin, Concrete Science, Hyden, 1981

[5] R. Defay, I. Prigogine, A. Bellemans and D. H. Everett, Surface Tension and Adsorption, Wiley, 1966

[6] S. Brunauer, J. Skalny, I. Odler, Complete pore structure analysis, Proc. Int. Symp. Pore Struct. Prop. Mater., 6 Vols., Academia, Prague, 1973, C3-C26

[7] D. H. Everett, and J. M. Haynes, The thermodynamics of fluid interfaces in a porous medium, Part I. General thermodynamic consideration. Zeitschrift für Physikalishe Chemie Neue Floge 82 (1972) 36-48

[8] S. Tada, M. Tanaka, Y. Matsunaga, Measurement of pore structure of aerated concrete, Proc. Beijing Int. Symp. Cem. Concr. 3 (1985) 384-393

[9] S. Tada, K. Watanabe, Dynamic determination of sorption isotherm of cement based materials, Cem. Concr. Res. 35 (2005) 2271-2277

[10] J. Hagymassy Jr., Pore Structure Analysis by Water Vapor Adsorption, Department of Chemistry, Ph.D. Thesis of Clarkson College of Technology, 1970

[11] C. D. Lawrence, Hardened cement paste pore structures from nitrogen and butane adsorption isotherms. Principles and Applications of Pore Structural Characterization, Proc. RILEM/CNR Int. Symp ., Milan, (1983) 339-363

[12] R. Sh. Mikhail, S. A. Selim, Adsorption of organic vapors in relation to pore structure of hardened cement paste. Highway Research Board Special Report 98, (1966) 123-134

[13] P. Pfeifer, D. Avnir, Chemistry of noninteger dimensions between two and three. 1. Fractal theory of heterogeneous surfaces, J. Chem. Phys. 79 (7) (1983) 3558-3565
[14] D. N. Winslow, The fractal nature of the surface of cement paste, Cem. Concr. Res. 15 (1985) 817-824,
[15] G. A. Niklasson, Adsorption on fractal structures: Application to cement materials, Cem. Conc. Res. 23 (1993) 1153-1158
[16] R. E. Beddoe, K. Lang, Effect of moisture on fractal dimension and specific surface of hardened cement paste by small-angle X-ray scattering, Cem. Concr. Res. 24 (1994) 605-612